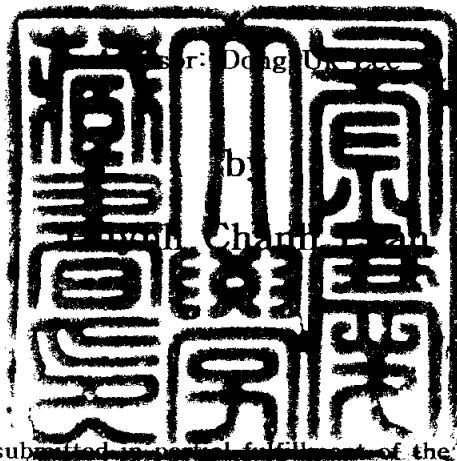


Thesis for the Degree of Master of Engineering

A Study of Stress Behavior on Welded Joint with Backing Strip

이면재 부착 용접이음부의
응력거동에 관한 연구



A thesis submitted in partial fulfillment of the requirements

for the Degree of
Master of Engineering

in the Department of Civil Engineering, Graduate School,
Pukyong National University

August 2004

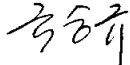
A Study of Stress Behavior on Welded Joint
with Backing Strip

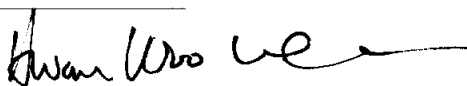
A Dissertation

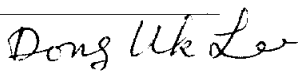
by

Huynh Chanh Luan

Approved as style and content by :

(Chairman) Seung Kyu Kook 

(Member) Hwan Woo Lee 

(Member) Dong Uk Lee 

23rd June 2004

CONTENTS

List of Illustrations	iv
List of Tables	vi
Abstract	vii

Chapter

1. INTRODUCTION	1
2. WELDED JOINTS WITH BACKING STRIP IN STEEL STRUCTURES	3
2.1 Welding Longitudinal Stiffeners of Steel Deck Bridge	3
2.1.1 Steel Bridge Deck Structure	3
2.1.2 Closed Rib Configuration	4
2.1.3 Closed rib field welded joint	6
2.2 Welding pipe structure with backing strip	7
2.2.1 Pipe connection position	7
2.2.2 Welding time in steel pipe structure	7
2.2.3 Weld defects and corrective actions	8
3. BASIC THEORY OF STRESS ANALYSIS IN FINITE ELEMENT METHOD	12
3.1 Stress analysis in FEM	12
3.2 Fundamental of elasticity mechanics	13

3.2.1 Stress equilibrium equation	13
3.2.2 Strain, displacement and compatibility equation . . .	16
3.2.3 Stress-strain relationship	17
3.2.4 Boundary conditions	19
3.2.5 Plane stress and plane strain	19
3.2.6 Stress-strain relationship	21
3.2.7 Boundary conditions	22
3.3 Two - Dimensional analysis	23
3.3.1 Formulation of FEM	23
3.3.2 Two dimensional condition	25
3.3.3 Plane stress analysis	26
4. STRESS ANALYSIS OF WELDED JOINT WITH BACKING STRIP	29
4.1 Case I : 8.0mm thick U rib	30
4.1.1 The relation between magnitude of misalignment and SCF	30
4.1.2 The relation between variation of root shape and stress concentration	33
4.1.3 The relation between root gap, backing strip's dimension and SCF	36
4.2 Case II : 6.0mm thick U rib	38
4.2.1 The relation between variation of misalignment and SCF	38
4.2.2 The relation between variation of root shape and SCF	39

4.2.3 The relation between root gap, backing strip's	
dimension and SCF	40
5. CONCLUSION	43
BIBLIOGRAPHIES	45
ACKNOWLEDGEMENTS	48

ILLUSTRATIONS

Figure	Page
2.1.1. Longitudinal Stiffeners of Steel Deck Bridge	3
2.1.2. The Transmission of Loads on Steel Deck Bridge	4
2.1.3. Standard Cross Section of Closed U Rib	5
2.1.4. U Rib Arrangement	5
2.1.5. Detailed Description of Field Welded Joint of U Rib	6
2.1.6. Front View of Field Welded Joint of U Rib	6
2.2.1. Misalignment at Field Weld Joint in Pipe Structure	8
2.2.2. Backing Strip Inserted Inside Pipe Structures at Field Welded Joint Positions	9
3.2.1. Element in Three Dimensional State of Stress	15
3.2.2. Plane Stress State	20
3.2.3. Plane Strain State	22
3.3.1. Nodal Displacements of Triangular Element in Plane Stress and Plane Strain State	23
3.3.2. Element in Plane Stress	26
3.3.3. Stresses Acting on the Wedge-Shaped Stress Element in Plane Stress	26
3.3.4. Geometry Represent of Eq. (3.54)	28
4.1.1. Cross Section of Welded Joint with Backing Strip	29
4.1.2. Analysis Model and Stress Distribution According to the Variation of Magnitude of Misalignment	31
4.1.3. Relation between Magnitude of Misalignment and	

SCF	32
4.1.4. Discretization of Discontinuity Region and Stress Distribution	35
4.1.5. Relation between Root Shape and SCF	35
4.1.6. Relation between the Variation of Root Gap and SCF	36
4.1.7. Relation between Backing Strip's Thickness and SCF	37
4.1.8. Relation between Backing Strip's Width and SCF	38
4.2.1. Relation between Magnitude of Misalignment and SCF	39
4.2.2. Relation between Root Shape and SCF	40
4.2.3. Relation between the Variation of Root Gap and SCF	41
4.2.4. Relation between Backing Strip's Thickness and SCF	42
4.2.5. Relation between Backing Strip's Width and SCF	42

TABLES

Table	Page
2.1. A Proposal of Standard Welding Time for Steel Pipe . . .	7
2.2. Weld Defects	10

A Study of Stress Behavior on Welded Joint with Backing Strip

Huynh Chanh Luan

Department of Civil Engineering, Graduate School

Pukyong National University

Abstract

The inaccurately assembly causes misalignment at field welded joint of U rib of steel bridge deck. Thus, a backing strip is attached to misalignment position so that welding can be performed under overhead position. However, misalignment at butt-welded joints induces bending stresses with the application of in plane loads only. This stress concentration will have a detrimental effect on ultimate strength and fatigue strength at the weld.

In the present study, finite element method is employed to investigate the relation of stress concentration factor (SCF) at discontinuity region to the variation of magnitude of misalignment, root shape, root gap and backing strip's dimension. Stress analysis is conducted for 2 cases: 8.0mm thick U rib and 6.0mm thick U rib.

It is found that stress concentration factor is not a constant, but varies with the magnitude of misalignment, root shape, root gap and backing strip's dimension. The bigger the magnitude of misalignment is, the bigger SCF is. However, backing strip's dimension has no much effect on SCF

CHAPTER I

INTRODUCTION

The use of steel bridges has increased in recent years because of their light self-weight, the developing of metallurgy and the emphasis on aesthetic considerations. Moreover, long span steel bridge emerges as an optimum choice for its advantageous such as light in weight of steel bridge deck, high in duration and saves up much time for constructing. Deck plate is reinforced by longitudinal and cross ribs, then the co-working of deck plate and longitudinal ribs do not form a high rigidity deck plate, is also considered as upper flange of main girder. Furthermore, cross ribs have complex function which are supporting to deck plate and working as cross stiffeners.

In long span bridge, open and closed section ribs are available but closed section ribs is much more popularity to be used as longitudinal stiffeners because of their high torsion resistance rigidity. Owing to using closed ribs, the longitudinal loads are redistributed uniformly, and we can lengthen the span of bridge. Beside, just one side welding need to be operated on closed section ribs, less deposited weld metal will be required and weld distorsion will reduce. In addition, the U section is perfectly closed, thereby helping to prevent any inner corrosion. Another advantage is that only the outer surface need painting, so the painting area is reduced.

When we erect a bridge, lower flange and webs are connected by bolts at first, then the deck plates relating to asphalt pavement are connected by welded joints, finally closed ribs are done by either bolts or welded joints. A long continuously welded joint somewhat causes a misalignment of U rib connection.

When the misalignment occurs we can also connect U ribs by bolts but bolts are stretched. When U ribs are connected by welded

joints, the misalignment creates an eccentric moment and position in which welding is performed from the under side of the joint (overhead position). The backing strips, which cause discontinuity, are attached to misalignment positions so that welding can be operated in overhead position.

In this paper, finite element method is used for stress analysis and the design of welded joint of closed ribs in steel box girder is covered by the design specifications. The stress analysis is conducted on closed rib having 6.0mm and 8.0mm thickness while magnitude of misalignment varies

CHAPTER II

WELDED JOINTS WITH BACKING STRIP IN STEEL STRUCTURES

2.1 Welding Longitudinal Stiffeners of Steel Deck Bridge

2.1.1 Steel Deck Bridge Structure

In figure 2.1.1, longitudinal and cross ribs are welded to deck plate. Deck plate is directly subjected to vehicle loads and then transmits them to longitudinal stiffeners. Deck plate and longitudinal stiffeners do not only play a role as bridge deck but as upper flange of main girder. Similarly, cross stiffeners do not reinforce deck plate but also work as floor beam

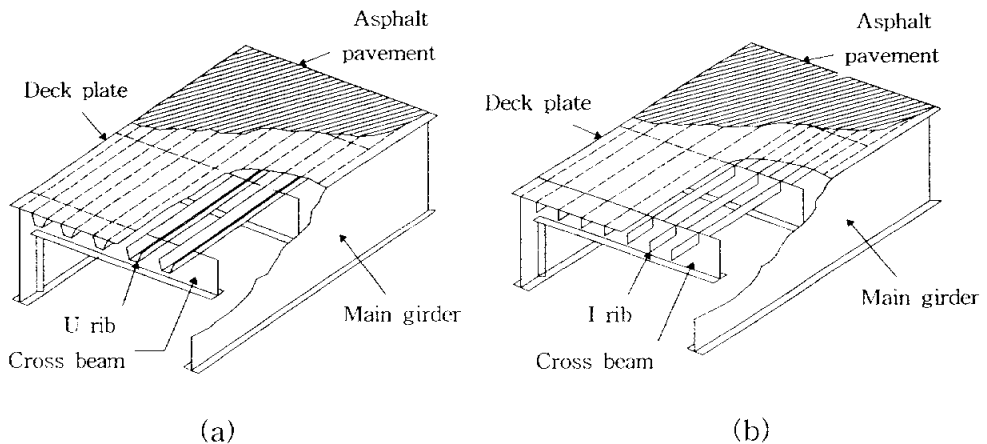


Figure 2.1.1. Longitudinal Stiffeners of Steel Deck Bridge :
a) Steel Bridge Deck Using Closed Section Longitudinal Stiffeners
b) Steel Bridge Deck Using Opened Section Longitudinal Stiffeners

As shown in figure 2.1.2 a concentrated load P applied to deck plate is distributed into two concentrated loads P_1 and P_2 at point E

and F. Then, P_1 is resolved into loads P_1' , P_1'' at intersection of longitudinal ribs and cross ribs (A and C). P_2 is resolved into loads P_2' , P_2'' at point B and D. Finally, these loads are transmitted to main girder through points G, I, K, M and points H, J, L, N.

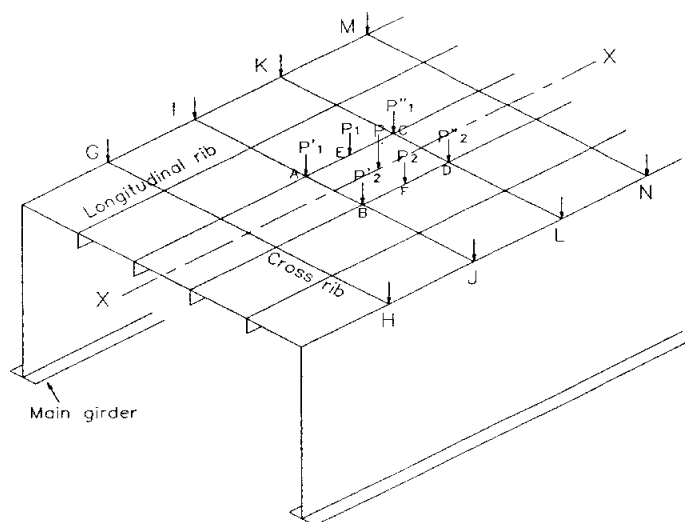


Figure 2.1.2. The Transmission of Loads on Steel Deck Bridge

2.1.2 Closed Rib Configuration

A standard closed U rib cross section is described as in figure 2.1.3. Because the inner part is completely enclosed, a half of area need prevented from corrosion. The torsion rigidity of closed U rib is governed by its own shape rather than its thickness. Consequently, the increasing of thickness doesn't result in much change of section properties.

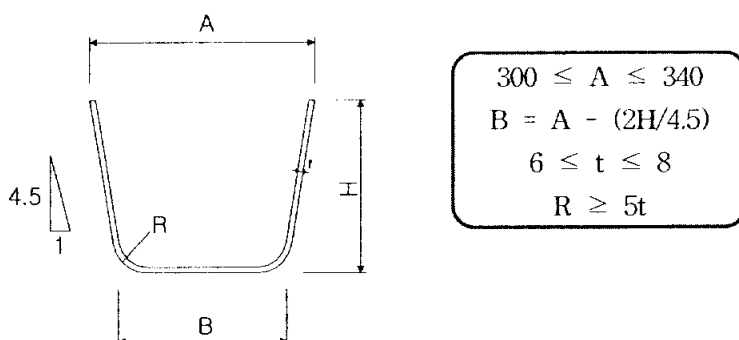


Figure 2.1.3. Standard Cross Section of Closed U Rib

According to domestic highway design criteria, the minimum allowable thickness is 8.0mm, but the minimum allowable thickness from 6.0 to 8.0mm is sometimes permissible for economic efficiency.

To avoid breaking asphalt pavement off due to bridge deck displacement, bridge deck rigidity must be large enough; the interval between longitudinal ribs and cross ribs should be limited. However, the smallest allowable interval between longitudinal ribs and cross ribs is dependent on practicability of field welded joint and bolt connection. As the result of that, the interval between longitudinal ribs in design is often in range from 150 to 200 mm. Figure 2.1.4 shows longitudinal closed rib's arrangement.

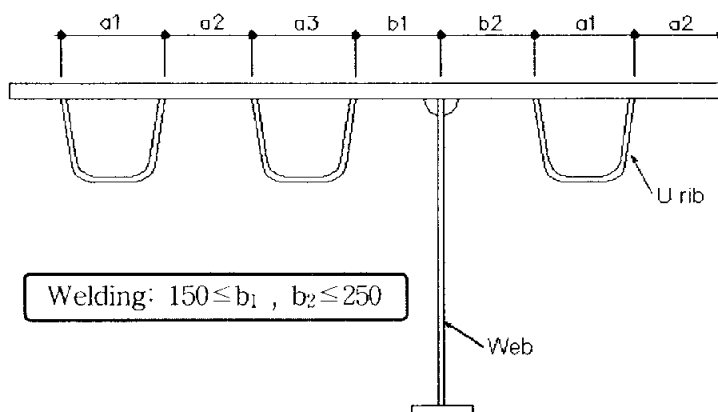


Figure 2.1.4. U Rib Arrangement

2.1.3 Closed rib field welded joint

Backing strip and diaphragm are attached to longitudinal rib at field welded joint position. Then a short section of closed rib is used to connect two ends of shop longitudinal ribs by butt welded joint. Figure 2.1.6 shows a front view of field welded joint of closed U rib.

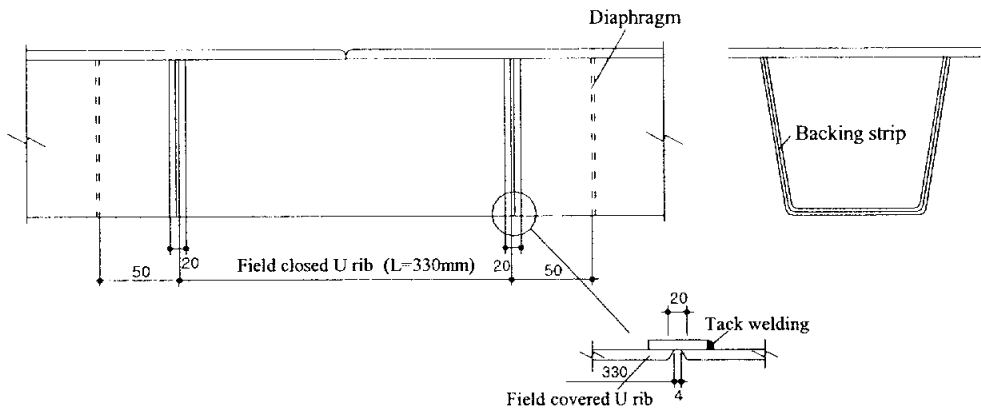


Figure 2.1.5. Detailed Description of Field Welded Joint of U Rib

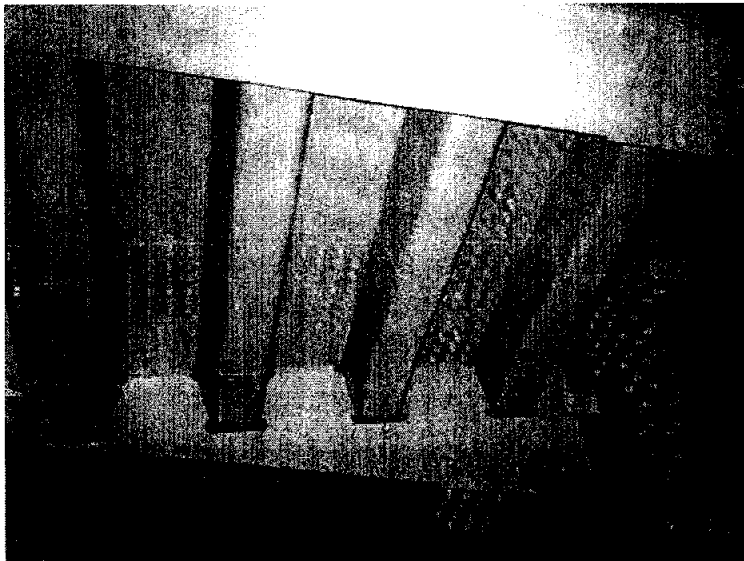


Figure 2.1.6. Front View of Field Welded Joint of U Rib

2.2 Welding pipe structure with backing strip

Steel pipe structures provide the most efficient cross-sectional shape under axial and lateral resistance ability. Because the number of welded joints are in proportion to length of pipe structures, we should increase factor of safety for field welded joint in steel pipe structures. Moreover, another reason is the manual method of applying is used for the greatest majority of pipe work at field than semi-automatic or automatic method.

2.2.1 Pipe connection position

We leave about 50~80cm away from field welded joint of lower pipe to make sure that the fitup of the joint is accurate. Then, construction is kept going after checking welding quality. If after 1 to 2 minutes, the welded joint is cooling down below 300°C, it will be less affected by harmful environment.

2.2.2 Welding time in steel pipe structure

We should reduce time spending on operating field welded joints. However, field welded joints have much effect on strength of steel pipe structures, we attempt to avoid weld effects as much as possible. Table 2.1. shows appropriate welding time for pipe structures

Table 2.1 A Proposal of Standard Welding Time for Steel Pipe.

Pipe size(mm)	$\phi 500 \times t9$	$\phi 500 \times t12$	$\phi 600 \times t12$	$\phi 1016 \times t14$
semi-automatic welding (min)	15~20	20~25	25~30	40~50
manual welding (min)	40~60	50~70	60~80	140~160

2.2.3 Weld defects and corrective action

Many kind of weld defects may occur due to welding conditions at field, so edge preparation, cleaning metal surface (remove rust or organic, oil dust), checking welding apparatus condition and damp electrode must be done before welding. Welding quality need to be check so that serious defects are detected and replaced in time. Figure 2.2.1 shows misalignment in pipe structures when fitting up upper and lower pipes. In figure 2.2.2, backing strip is attached to inside pipe work at field welded joint. Weld defects, probable causes, and corrective actions are tabulated in Table 2.2.

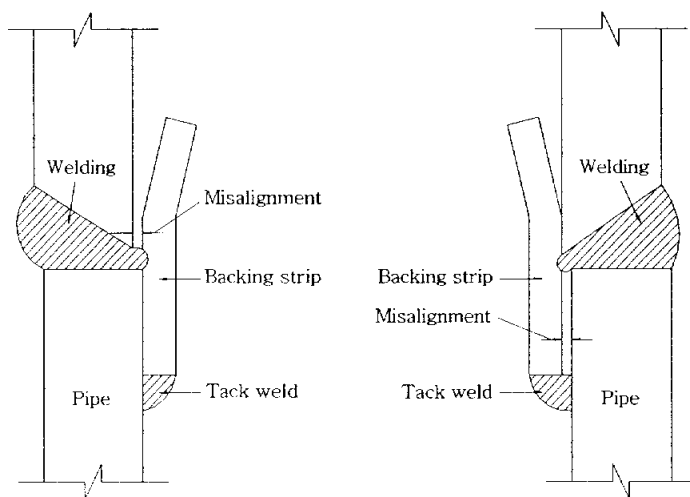


Figure 2.2.1. Misalignment at Field Welded Joint in Pipe Structure

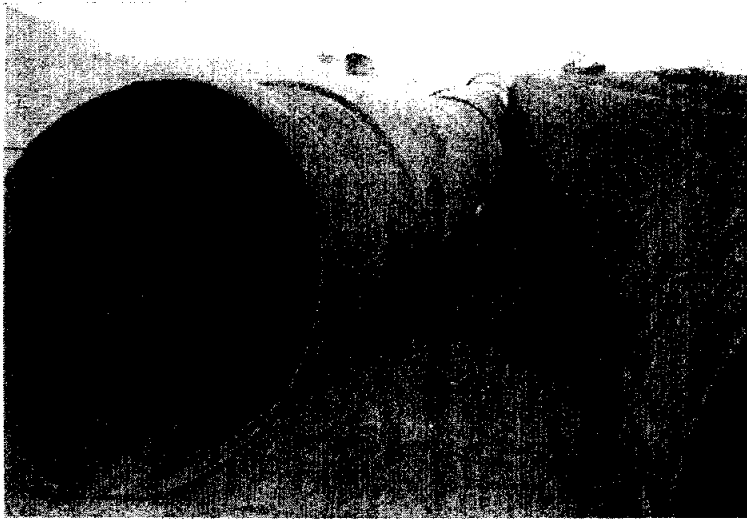


Figure 2.2.2. Backing Strip Inserted Inside Pipe Structures
at Field Welded Joint Positions

Table 2.2 Weld Defects

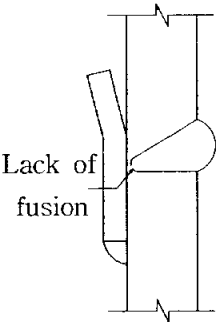
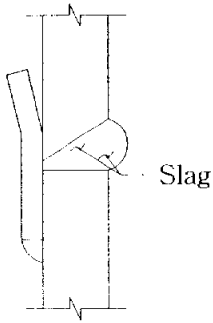
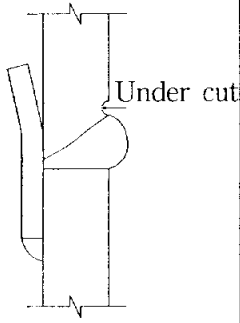
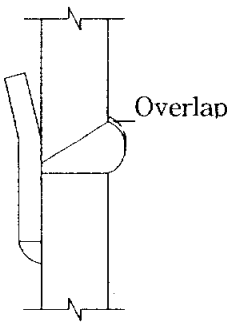
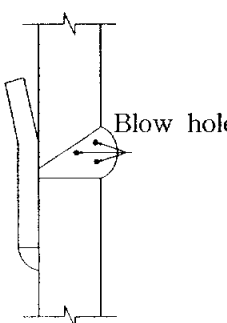
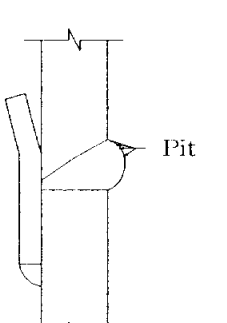
Defect	Probable cause	Corrective action
<p>Lack of fusion</p>  <p>The diagram shows a cross-section of a butt joint. The weld metal is shown on the left, and the root opening is on the right. The weld metal does not fully fuse with the root, leaving a gap. The label 'Lack of fusion' is placed next to the gap.</p>	<ol style="list-style-type: none"> 1. Root opening too small 2. Welding speed too fast 3. Welding current too low 4. Improper torch angle 	<ol style="list-style-type: none"> 1. Design root opening about 1~4mm 2. Control welding speed 3. Keep maximum current about 450A 4. Welding with torch angle about 20°~30°
<p>Slag inclusion</p>  <p>The diagram shows a cross-section of a butt joint. The weld metal is shown on the left, and the root opening is on the right. A line points to a dark, irregular shape within the weld metal, labeled 'Slag'.</p>	<ol style="list-style-type: none"> 1. Remove slag incompletely 2. Welding speed too low 3. Utilize forehand welding technique 	<ol style="list-style-type: none"> 1. Remove slag completely 2. Increase welding current and control slag floating speed 3. Utilize back hand welding technique with torch angle about 0~45°
<p>Under cut</p>  <p>The diagram shows a cross-section of a butt joint. The weld metal is shown on the left, and the root opening is on the right. A line points to a sharp, V-shaped groove at the toe of the weld, labeled 'Under cut'.</p>	<ol style="list-style-type: none"> 1. Welding current too high 2. Incorrect torch angle for welding position 3. Welding speed too fast 4. Arc voltage too high 	<ol style="list-style-type: none"> 1. Decrease welding current in range of 350~400A 2. Keep torch angle in range 0~15° and aim torch at bevel of upper pipe 3. Control welding speed corresponding to deposition rate 4. Decrease arc voltage about 26~28V

Table 2.2 Weld Defects (cont.)

Defect	Probable cause	Corrective action
Overlap 	<ol style="list-style-type: none"> 1. Welding current too low 2. Torch travel speed too low 	<ol style="list-style-type: none"> 1. Increase welding current for welding faster 2. Increase torch travel speed
Porosity 	<ol style="list-style-type: none"> 1. Arc voltage low 2. Welding over moisture surface and foreign material 3. Damp electrode 4. Protruding electrode wire too short 	<ol style="list-style-type: none"> 1. Reasonable voltage : 26~30V 2. Clean weld area and keep clean 3. Properly storage electrode and use fresh dry electrode 4. Control electrode wire protrude about 20~50mm
Cavities / Pit 	<ol style="list-style-type: none"> 1. Damp electrode 2. Welding over moisture surface and foreign material 3. Improper welding current and voltage 	<ol style="list-style-type: none"> 1. Properly storage electrode and use fresh dry electrode 2. Clean weld area, remove rust and dust before welding 3. Utilize correct welding technique for electrode type and joint design

CHAPTER III

BASIC THEORY OF STRESS ANALYSIS IN FINITE ELEMENT METHOD

3.1 Stress analysis in FEM

The finite element method is a numerical method for solving engineering and mathematical physics problems. In this method, a body is divided into a finite smaller elements which is interconnected at common points of two or more elements and/or boundary lines and/or surface. In stead of solving the problem for the entire body, we formulate the equations for each finite element and combine them to obtain the solution of the whole body. The general procedure in a FEM of an elastic problem will be illustrated in the following steps:

1. We divide body into an equivalent system of finite elements with common nodes. The choice of size and type of elements used in finite element analysis depends on boundary and loading conditions.
2. We select a displacement function with each element. The function is defined within the element using the nodal values of the element. Moreover, displacement must satisfy the continuity at common nodes of elements.
3. Strain-displacement and stress-strain relationships are defined for deriving the equations for each finite element.
4. Then, from above relationship element stiffness matrices are obtained by using direct equilibrium method or energy method etc.,
5. The individual element equations can be added together to obtain the global equations for the whole structure.
6. Now, we must apply certain boundary conditions so that the

structure remains in place instead of moving as a rigid body. Moreover, the applied known loads have been accounted for in the global force matrix.

7. We solve system of n equations for the n unknown degrees of freedom by using elimination method or iterative method.

8. Finally, stress-strain and strain-displacement relationship help with determine structural stresses and displacements.

3.2 Fundamental of elasticity mechanics

3.2.1 Stress equilibrium equation

A point in a body is generally in three dimensional state of stress. Figure 3.2.1 shows an infinitesimal cube having sides of lengths dx , dy , dz in the x , y , z directions, respectively. Stresses acting on element are as following

$$\{\sigma\}^T = [\sigma_x \sigma_y \sigma_z \tau_{xy} \tau_{yz} \tau_{zx}] \quad (3.1)$$

Where

$$\tau_{xy} = \tau_{yx}, \quad \tau_{yz} = \tau_{zy}, \quad \tau_{zx} = \tau_{xz}$$

$\sigma_x, \sigma_y, \sigma_z$: act in direction perpendicular to the surface of material

$\tau_{xy}, \tau_{yz}, \tau_{zx}$: act tangential to the surface of the material

In equation 3.1, subscript T means transpose matrix

$$T = \begin{bmatrix} \sigma_x & \tau_{yx} & \tau_{zx} \\ \tau_{xy} & \sigma_y & \tau_{zy} \\ \tau_{xz} & \tau_{yz} & \sigma_z \end{bmatrix} \quad T' = \begin{bmatrix} \sigma'_x & \tau'_{yx} & \tau'_{zx} \\ \tau'_{xy} & \sigma'_y & \tau'_{zy} \\ \tau'_{xz} & \tau'_{yz} & \sigma'_z \end{bmatrix} \quad (3.2)$$

Equation 3.2 shows the state of stress at a point along with OXYZ and OX'Y'Z' coordinate system. The OXYZ and OX'Y'Z' coordinate systems are related by the following equation:

$$T = L T' L^T \quad (3.3)$$

where

$$L = \begin{bmatrix} l_1 & m_1 & n_1 \\ l_2 & m_2 & n_2 \\ l_3 & m_3 & n_3 \end{bmatrix} \quad (3.4)$$

$(l_1, m_1, n_1), (l_2, m_2, n_2), (l_3, m_3, n_3)$ are direction cosines
 and $l_1 = \cos(x', x), m_1 = \cos(x', y), n_1 = \cos(x', z)$
 $l_2 = \cos(y', x), m_2 = \cos(y', y), n_2 = \cos(y', z)$
 $l_3 = \cos(z', x), m_3 = \cos(z', y), n_3 = \cos(z', z)$

There are three planes of zero shear stress exist, that these planes are mutually perpendicular, and that on these planes the normal stresses have maximum and minimum values. These normal stresses are referred to as principle stresses.

The principle stresses are the three roots of the following relationship:

$$\begin{vmatrix} \sigma_x - \sigma & \tau_{yx} & \tau_{zx} \\ \tau_{xy} & \sigma_y - \sigma & \tau_{zy} \\ \tau_{xz} & \tau_{yz} & \sigma_z - \sigma \end{vmatrix} = 0 \quad (3.5)$$

Principle stresses are usually denoted as $\sigma_1, \sigma_2, \sigma_3$ ($\sigma_1 \geq \sigma_2 \geq \sigma_3$). We have

$$\left. \begin{aligned} J_1 &= \sigma_x + \sigma_y + \sigma_z = \sigma_1 + \sigma_2 + \sigma_3 \\ J_2 &= \sigma_x \sigma_y + \sigma_y \sigma_z + \sigma_z \sigma_x - \tau_{xy}^2 - \tau_{yz}^2 - \tau_{zx}^2 \\ &= \sigma_1 \sigma_2 + \sigma_2 \sigma_3 + \sigma_3 \sigma_1 \\ J_3 &= \sigma_x \sigma_y \sigma_z + 2 \tau_{xy} \tau_{yz} \tau_{zx} - \sigma_x \tau_{yz}^2 - \sigma_y \tau_{zx}^2 \\ &\quad - \sigma_z \tau_{xy}^2 = \sigma_1 \sigma_2 \sigma_3 \end{aligned} \right\} \quad (3.6)$$

It follows from equation 3.6 that the coefficients J_1, J_2, J_3 are independent of coordinate systems.

When we choose coordinate system having axes coincide with principle stresses direction

$$\{\sigma\}^T = [\sigma_1 \ \sigma_2 \ \sigma_3 \ 0 \ 0 \ 0] \quad (3.7)$$

The differential equations of equilibrium for an infinitesimal shown in figure 3.2.1 :

$$\left. \begin{aligned} \frac{\partial \sigma_x}{\partial x} + \frac{\partial \tau_{xy}}{\partial y} + \frac{\partial \tau_{zx}}{\partial z} + X' &= 0 \\ \frac{\partial \tau_{xy}}{\partial x} + \frac{\partial \sigma_y}{\partial y} + \frac{\partial \tau_{yz}}{\partial z} + Y' &= 0 \\ \frac{\partial \tau_{zx}}{\partial x} + \frac{\partial \tau_{yz}}{\partial y} + \frac{\partial \sigma_z}{\partial z} + Z' &= 0 \end{aligned} \right\} \quad (3.8)$$

Where X', Y', Z' are components of body force per unit volume

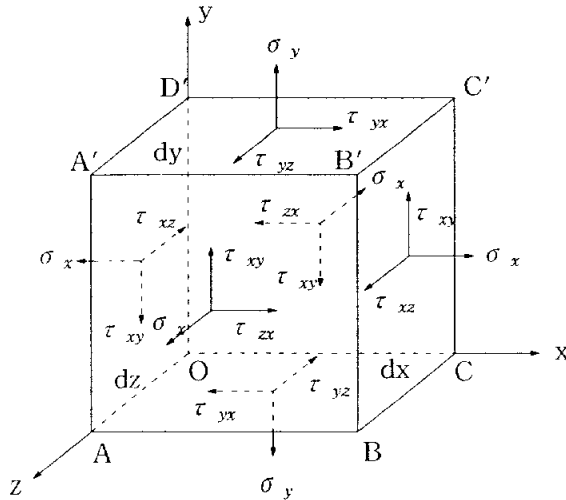


Figure 3.2.1. Element in Three Dimensional State of Stress

3.2.2 Strain, displacement and compatibility equation

Following with 6 components of stress in equation 3.1, there are also 6 components of strain

$$\{\epsilon\}^T = [\epsilon_x \quad \epsilon_y \quad \epsilon_z \quad \gamma_{xy} \quad \gamma_{yz} \quad \gamma_{zx}] \quad (3.9)$$

Where $\epsilon_x, \epsilon_y, \epsilon_z$ are normal strain components

$\gamma_{xy}, \gamma_{yz}, \gamma_{zx}$ are shearing strain components

When coordinate axes coincide with principle directions, we have

$$\{\epsilon\}^T = [\epsilon_1 \quad \epsilon_2 \quad \epsilon_3 \quad 0 \quad 0 \quad 0] \quad (3.10)$$

Similarly, the relation of principle strain to $\epsilon_x, \epsilon_y, \epsilon_z, \gamma_{xy}, \gamma_{yz}, \gamma_{zx}$ are as following

$$\left. \begin{aligned} I_1 &= \epsilon_x + \epsilon_y + \epsilon_z = \epsilon_1 + \epsilon_2 + \epsilon_3 \\ I_2 &= \epsilon_x \epsilon_y + \epsilon_y \epsilon_z + \epsilon_z \epsilon_x - (\gamma_{xy}^2 + \gamma_{yz}^2 + \gamma_{zx}^2)/4 \\ &= \epsilon_1 \epsilon_2 + \epsilon_2 \epsilon_3 + \epsilon_3 \epsilon_1 \\ I_3 &= \epsilon_x \epsilon_y \epsilon_z + (\gamma_{xy} \gamma_{yz} \gamma_{zx} - \epsilon_x \gamma_{yz}^2 - \epsilon_y \gamma_{zx}^2 - \epsilon_z \gamma_{xy}^2)/4 \\ &= \epsilon_1 \epsilon_2 \epsilon_3 \end{aligned} \right\} \quad (3.11)$$

The strain at a point can be decomposed into two components: dilatational strain ϵ_v and deviator strain ϵ_d

$$\left. \begin{aligned} \{\epsilon\}^T &= \{\epsilon_v\}^T + \{\epsilon_d\}^T \\ \{\epsilon_v\}^T &= [I_1/3 \quad I_1/3 \quad I_1/3 \quad 0 \quad 0 \quad 0] \\ \{\epsilon_d\}^T &= [\epsilon_x - I_1/3 \quad \epsilon_y - I_1/3 \quad \epsilon_z - I_1/3 \quad \gamma_{xy} \quad \gamma_{yz} \quad \gamma_{zx}] \\ &= [\epsilon_{dx} \quad \epsilon_{dy} \quad \epsilon_{dz} \quad \gamma_{xy} \quad \gamma_{yz} \quad \gamma_{zx}] \end{aligned} \right\} \quad (3.12)$$

Now, the small displacement of particles of a deformed body will be resolved into components u, v, w parallel to the coordinate axes x, y, z , respectively.

$$u = ui + vj + wk \quad (3.13)$$

where i, j, k are unit vectors along x, y, z direction, respectively

The strain-displacement relationships are defined as follows:

$$\left. \begin{aligned} \epsilon_x &= \frac{\partial u}{\partial x}, \quad \epsilon_y = \frac{\partial v}{\partial y}, \quad \epsilon_z = \frac{\partial w}{\partial z} \\ \gamma_{xy} &= \frac{\partial v}{\partial x} + \frac{\partial u}{\partial y} \\ \gamma_{yz} &= \frac{\partial w}{\partial y} + \frac{\partial v}{\partial z}, \\ \gamma_{zx} &= \frac{\partial u}{\partial z} + \frac{\partial w}{\partial x} \end{aligned} \right\} \quad (3.14)$$

Six components of strain at each point are completely determined by three components of displacement u, v, w . Therefore, components of strain cannot be arbitrarily specified as functions of x, y and z . The strains are not independent of one another, and their relations are known as compatibility conditions.

3.2.3 Stress-strain relationship

Hooke's law shows the linear relationship between stress and strain. For a three-dimensional state of stress, each of the six stress components is expressed as a linear function of six components of strain within the linear elastic range, and vice versa. We express Hooke's law for any homogenous elastic material as follows:

$$\{ \sigma \} = [d_{ij}] \{ \epsilon \} = [D] \{ \epsilon \} \quad (3.15)$$

Similarly

$$\{ \varepsilon \} = [C] \{ \sigma \} = [C] \{ \sigma \} \quad (3.16)$$

[D] and [C] are symmetric matrices

In case of anisotropic elastic material, we have

$$\left[\begin{array}{l} \varepsilon_x = \frac{\sigma_x}{E_x} - \frac{\nu_{yx}}{E_y} \sigma_y - \frac{\nu_{zx}}{E_z} \sigma_z \\ \varepsilon_y = -\frac{\nu_{xy}}{E_x} \sigma_x + \frac{\sigma_y}{E_y} - \frac{\nu_{zy}}{E_z} \sigma_z \\ \varepsilon_z = -\frac{\nu_{xz}}{E_x} \sigma_x - \frac{\nu_{yz}}{E_y} \sigma_y + \frac{\sigma_z}{E_z} \\ \gamma_{xy} = \frac{\tau_{xy}}{G_{xy}}, \gamma_{yz} = \frac{\tau_{yz}}{G_{yz}}, \gamma_{zx} = \frac{\tau_{zx}}{G_{zx}} \end{array} \right] \quad (3.17)$$

In equation 3.17, there are 12 constants but the number of independent constants are 9.

If material is isotropic, the number of independent constants reduces to 2. Therefore, matrices [C] and [D] are expressed in terms of modulus elastic E, Poisson ratio ν .

$$[C] = \left[\begin{array}{ccccccc} 1/E & -\nu/E & -\nu/E & 0 & 0 & 0 \\ & 1/E & -\nu/E & 0 & 0 & 0 \\ & & 1/E & 0 & 0 & 0 \\ & & & 2(1+\nu)/E & 0 & 0 \\ & & & & 2(1+\nu)/E & 0 \\ & & & & & 2(1+\nu)/E \end{array} \right] \quad (3.18)$$

symmetric

$$[D] = \frac{E}{(1+\nu)(1-2\nu)} \left[\begin{array}{ccccccc} 1-\nu & \nu & \nu & 0 & 0 & 0 \\ & 1-\nu & \nu & 0 & 0 & 0 \\ & & 1-\nu & 0 & 0 & 0 \\ & & & (1-2\nu)/2 & 0 & 0 \\ & & & & (1-2\nu)/2 & 0 \\ & & & & & (1-2\nu)/2 \end{array} \right] \quad (3.19)$$

symmetric

3.2.4 Boundary conditions

We assume that external surface forces act on part S_1 of the boundary and displacements on part S_2 of the boundary.

Denote the components of the surface forces per unit area at a point under consideration as:

$$X_\nu = X'_\nu, Y_\nu = Y'_\nu, Z_\nu = Z'_\nu; \text{ on } S_1 \quad (3.20)$$

$$\begin{Bmatrix} X_\nu \\ Y_\nu \\ Z_\nu \end{Bmatrix} = \begin{bmatrix} \sigma_x & \tau_{xy} & \tau_{zx} \\ \tau_{xy} & \tau_y & \tau_{yz} \\ \tau_{zx} & \tau_{yz} & \tau_z \end{bmatrix} \begin{Bmatrix} l \\ m \\ n \end{Bmatrix} \quad (3.21)$$

in which l, m, n are the direction cosines of the external normal to the surface of the body at the point under consideration

The boundary displacements per unit area are defined as follows:

$$u = u', v = v', w = w'; \text{ on } S_2 \quad (3.22)$$

The system of equations including equations of equilibrium and boundary conditions is generally sufficient for determining the stress components. In addition, if the stress components satisfy equations of compatibility, this stress system is the correct solution of the problem.

3.2.5 Plane stress and plane strain

In some special load and boundary conditions, a body in three dimensional state of stress can be approximately treated as in two dimensional state of stress. Two dimensional state of stress refer to plane stress and plane strain

1) Plane stress

A thin plate is loaded by forces uniformly distributed over the thickness, parallel to the plane of the plate. Thus, the stress components in z direction ($\sigma_z, \tau_{xz}, \tau_{yz}$) are zero on both faces of plate:

$$\sigma_z = \tau_{xz} = \tau_{yz} = 0 \quad (3.23)$$

And we assume these stresses are also zero within the plate. The state of stress is specified by non zero stress components which are functions of x and y , only. This state of stress is called plane stress.

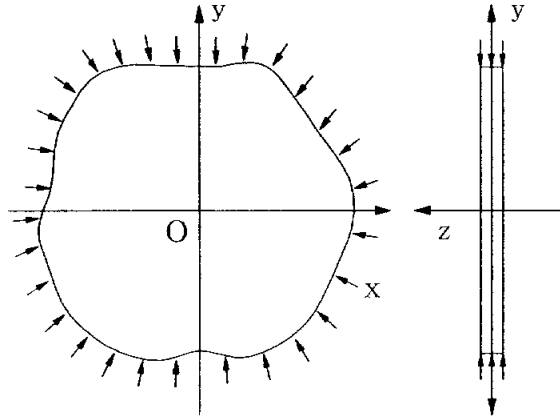


Figure 3.2.2. Plane Stress State

2) Plane strain

A long prismatic body subject to lateral loads and do not vary along the length as shown in figure 3.2.3. At a certain distance away from both ends, the components u and v of displacement are functions of x and y only and w component is zero. Thus,

$$\epsilon_z = \gamma_{xz} = \gamma_{yz} = 0 \quad (3.24)$$

Substitute equation 3.24 into equilibrium equations, strain-displacement relationship and compatibility equation:

(1) Equilibrium equations

$$\frac{\partial \sigma_x}{\partial x} + \frac{\partial \tau_{xy}}{\partial y} + X = 0, \quad \frac{\partial \tau_{xy}}{\partial x} + \frac{\partial \sigma_y}{\partial y} + Y = 0 \quad (3.25)$$

(2) And strain-displacement relationships:

$$\epsilon_x = \frac{\partial u}{\partial x}, \quad \epsilon_y = \frac{\partial v}{\partial y}, \quad \gamma_{xy} = \frac{\partial u}{\partial y} + \frac{\partial v}{\partial x} \quad (3.26)$$

(3) Compatibility equation

$$\frac{\partial^2 \epsilon_x}{\partial y^2} + \frac{\partial^2 \epsilon_y}{\partial x^2} = \frac{\partial^2 \gamma_{xy}}{\partial x \partial y} \quad (3.27)$$

3.2.6 Stress-strain relationship

1) Plane stress condition

$$\epsilon_x = (\sigma_x - \nu \sigma_y) / E, \quad \epsilon_y = (\sigma_y - \nu \sigma_x) / E, \quad \gamma_{xy} = \tau_{xy} / G \quad (3.28)$$

$$\text{Or} \quad \begin{Bmatrix} \sigma_x \\ \sigma_y \\ \tau_{xy} \end{Bmatrix} = \frac{E}{1 - \nu^2} \begin{bmatrix} 1 & \nu & 0 \\ \nu & 1 & 0 \\ 0 & 0 & (1 - \nu)/2 \end{bmatrix} \begin{Bmatrix} \epsilon_x \\ \epsilon_y \\ \gamma_{xy} \end{Bmatrix} \quad (3.29)$$

We set $\sigma_z, \tau_{yz}, \tau_{zx}$ are zero results in the follows:

$$\begin{aligned} \gamma_{yz} &= \gamma_{zx} = 0 \\ \epsilon_z &= -\frac{\nu}{1 - \nu} (\epsilon_x + \epsilon_y) \end{aligned} \quad (3.30)$$

2) Plane strain condition

Substituting ($\epsilon_z = 0$) results in the following relationships for plane strain condition:

$$\left. \begin{aligned} \epsilon_x &= [(1 - \nu^2) \sigma_x - \nu (1 + \nu) \sigma_y] / E \\ \epsilon_y &= [(1 - \nu^2) \sigma_y - \nu (1 + \nu) \sigma_x] / E \\ \gamma_{xy} &= \frac{\tau_{xy}}{G} \end{aligned} \right\} \quad (3.31)$$

Similarly,

$$\begin{Bmatrix} \sigma_x \\ \sigma_y \\ \tau_{xy} \end{Bmatrix} = \frac{E}{(1+\nu)(1-2\nu)} \begin{bmatrix} 1-\nu & \nu & 0 \\ \nu & 1 & 0 \\ 0 & 0 & (1-\nu)/2 \end{bmatrix} \begin{Bmatrix} \varepsilon_x \\ \varepsilon_y \\ \gamma_{xy} \end{Bmatrix} \quad (3.32)$$

Shearing stress $\tau_{yz} = \tau_{xz} = 0$

But $\sigma_z = \nu (\sigma_x + \sigma_y)$ (3.33)

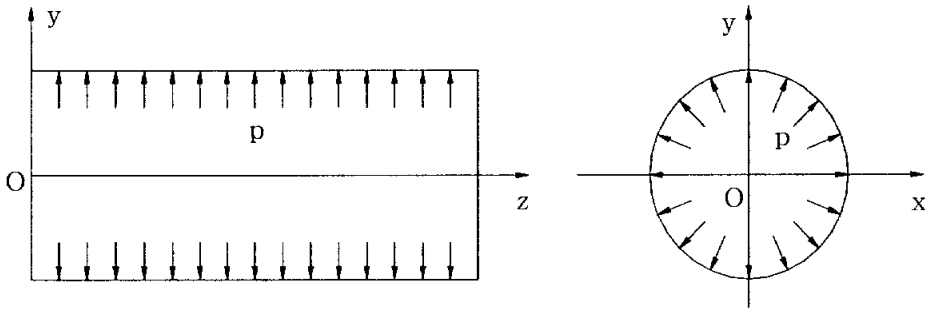


Figure 3.2.3. Plane Strain State

3.2.7 Boundary conditions

$$\sigma_x l + \tau_{xy} m = X'_\nu, \quad \tau_{xy} l + \sigma_y m = Y'_\nu \quad (3.34)$$

In the two-dimensional problems, the equations of equilibrium, together with those of compatibility and boundary conditions, provide a system of equations sufficient for determination of the complete stress distribution. It is shown that a solution satisfying this system of equations is unique.

3.3 Two-Dimensional analysis

We consider the triangular element, with nodes such as i, j and m in figure 3.3.1

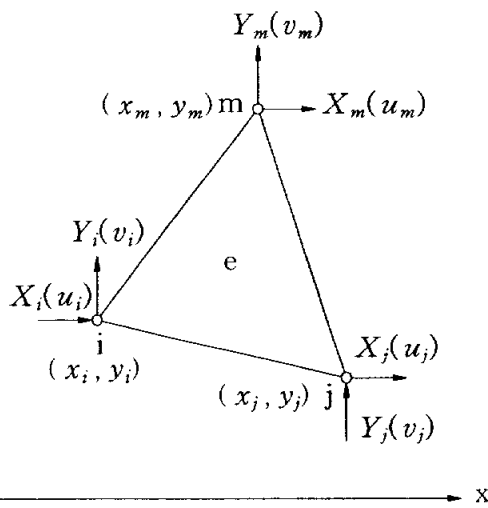


Figure 3.3.1. Nodal Displacements of Triangular Element in Plane Stress and Plane Strain State

3.3.1. Formulation of FEM

We select displacement function for each element as

$$\{f(x, y)\} = \begin{Bmatrix} u(x, y) \\ v(x, y) \end{Bmatrix} = [N]\{\delta\}^e = [N_i N_j N_m] \begin{Bmatrix} \delta_i \\ \delta_j \\ \delta_m \end{Bmatrix} \quad (3.35)$$

Where $[N]$ is shape functions matrix, functions of nodal coordinates, $\{\delta\}^e$ is nodal displacement of element e . δ_i implies u_i and v_i displacement components of node i in x and y directions. We assemble nodal displacements of all of elements

$$\{\delta\} = [\delta_1 \delta_2 \dots \delta_n]^T \quad (3.36)$$

We express the element strains in terms of the unknown nodal displacements.

$$\{ \varepsilon \} = \begin{Bmatrix} \varepsilon_x \\ \varepsilon_y \\ \gamma_{xy} \end{Bmatrix} = \begin{Bmatrix} \frac{\partial u}{\partial x} \\ \frac{\partial v}{\partial y} \\ \frac{\partial u}{\partial y} + \frac{\partial v}{\partial x} \end{Bmatrix} = [B] \{ \delta \}^e \quad (3.37)$$

[B] is generally function of the variable x, y and nodal coordinates, and [B] relates to N_i, N_j, N_m

In the some cases, nodal strains primarily receive certain values due to temperature or contraction. Stress-strain relationship for an elastic body:

$$\{ \sigma \} = [\sigma_x \sigma_y \tau_{xy}]^T = [D](\{ \varepsilon \} - \{ \varepsilon_0 \}) \quad (3.38)$$

[D] is matrix containing material property constants

Total load system on an element e includes:

$$\{ f \}^e = \int \int_V [N]^T \{ X \} dV + \{ P \} + \int \int_S [N_s]^T \{ T_s \} dS \quad (3.39)$$

(1) Concentrated nodal forces {P}

(2) Equivalent nodal forces from distributed loads or surface tractions

$$\int \int_S [N_s]^T \{ T_s \} dS \quad (3.40)$$

$[N_s]$ represents the shape function matrix evaluated along the surface where the surface traction acts

$\{ T_s \}$ represents the surface tractions

(3) Body forces

$$\int \int_V [N]^T \{X\} dV \quad (3.41)$$

$\{X\}$ is the body weight/unit volume or weight density matrix

Total load system relates to unknown nodal displacements $\{\delta\}^e$ as follows:

$$\{f\}^e = [k]^e \{\delta\}^e \quad (3.42)$$

where stiffness matrix $[k]^e$ of element e

$$[k]^e = \int \int_V [B]^T [D] [B] dV \quad (3.43)$$

We obtain the global structure stiffness matrix $[K]$ and equations by superposition each element stiffness matrix and equations

$$[K] = \sum_{e=1}^N [k]^e \quad (3.44)$$

$$\text{And } \{F\} = [K] \{d\} \quad (3.45)$$

$$\text{Where } \{F\} = \sum_{e=1}^N \{f\}^e \quad (3.46)$$

We determine the unknown global structure nodal displacements by solving the equation

$$\{\delta\} = [K]^{-1} \{F\} \quad (3.47)$$

Finally, nodal stresses is determined by stress-strain relationship (Hooke' law)

3.3.2 Two dimensional condition

In case of two dimensional condition (plane stress, plane strain), stress strain relationship is given by Eq 3.28 to Eq.3.33. And each node has 2 DOFs-an x and a y displacement.

3.3.3 Plane stress analysis

Figure 3.3.2 shows normal and shearing stresses acting on a rectangular plane stress element.

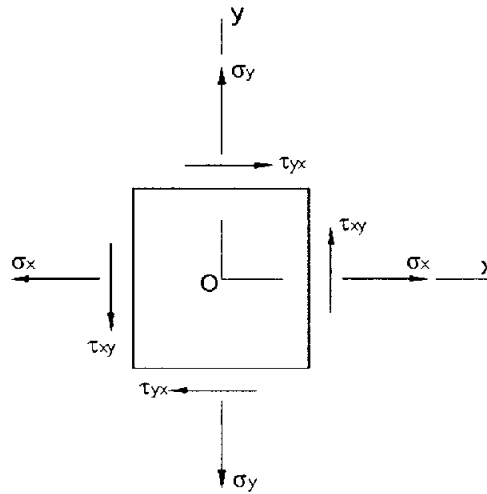


Figure 3.3.2. Element in Plane Stress

We now consider the stresses acting on inclined sections. For this purpose, we choose a triangular stress element having an inclined face and other two side faces parallel to the x and y axis, figure 3.3.3.

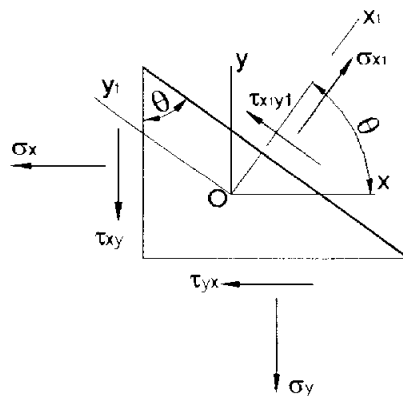


Figure 3.3.3. Stresses Acting on the Wedge-Shaped Stress Element in Plane Stress.

We obtain equations of equilibrium by summing forces in x and y direction

$$\sum H = 0: \sigma' ds \cos \theta + \tau' ds \sin \theta - \sigma_x dy - \tau_{yx} dx = 0 \quad (3.48)$$

$$\sum V = 0: \sigma' ds \sin \theta - \tau' ds \cos \theta - \sigma_y dx - \tau_{xy} dy = 0 \quad (3.49)$$

Substituting $\tau_{xy} = \tau_{yx}$, $dx = ds \sin \theta$ and $dy = ds \cos \theta$ into above equation and eliminating ds .

Then (Eq. 3.48) + (Eq. 3.49) $\times \sin \theta / \cos \theta$, we obtain:

$$\sigma' = \sigma_x \sin^2 \theta + \sigma_y \cos^2 \theta + 2 \tau_{xy} \sin \theta \cos \theta \quad (3.50)$$

And (Eq. 3.49) - (Eq. 3.48) $\times \cos \theta / \sin \theta$, we obtain:

$$\tau' = -(\sigma_x - \sigma_y) \sin \theta \cos \theta + \tau_{xy} (\cos^2 \theta - \sin^2 \theta) \quad (3.51)$$

The stresses on an inclined section can be expressed in a more convenient form by introducing the trigonometric identities:

$$\cos^2 \theta = \frac{1}{2}(1 + \cos 2\theta) \quad \sin^2 \theta = \frac{1}{2}(1 - \cos 2\theta)$$

$$\sin \theta \cos \theta = \frac{1}{2} \sin 2\theta$$

The equations become:

$$\sigma' = \frac{\sigma_x + \sigma_y}{2} + \frac{\sigma_x - \sigma_y}{2} \cos 2\theta + \tau_{xy} \sin 2\theta \quad (3.52)$$

$$\tau' = \frac{\sigma_x - \sigma_y}{2} \sin 2\theta + \tau_{xy} \cos 2\theta \quad (3.53)$$

The maximum and minimum normal stresses can be found by taking derivative of σ' with respect to θ and setting it equal to zero. The equation for the derivative is

$$d\sigma'/d\theta = (\sigma_x - \sigma_y) \sin 2\theta + 2\tau_{xy} \cos 2\theta \quad (3.54)$$

And

$$\tan 2\theta_p = \frac{2\tau_{xy}}{\sigma_x - \sigma_y} \quad (3.55)$$

$$\theta_p = \frac{1}{2} \tan^{-1} \frac{\tau_{xy}}{\sigma_y - \sigma_x} + \frac{n\pi}{2} \quad (3.56)$$

The angle θ_p has two values that differ by 90° , one value between 0 and 90° and the other between 90° and 180° . The two values of θ_p are known as the principle angle.

We introduce the expressions for $\cos 2\theta_p$ and $\sin 2\theta_p$:

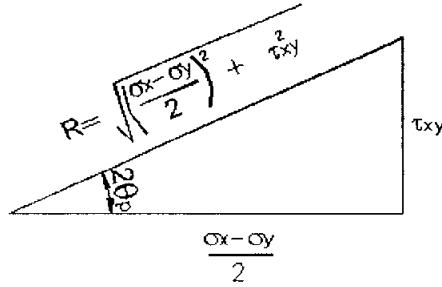


Figure 3.3.4. Geometry Represent of Eq. (3.54)

$$\cos 2\theta_p = \frac{\sigma_x - \sigma_y}{2R} \quad \sin 2\theta_p = \frac{\tau_{xy}}{R} \quad (3.57)$$

And substituting these expressions into equation 3.51, we obtain

$$\sigma_{\max} = \frac{\sigma_x + \sigma_y}{2} + \left[\left(\frac{\sigma_x - \sigma_y}{2} \right)^2 + \tau_{xy}^2 \right]^{1/2} \quad (3.58)$$

$$\sigma_{\min} = \frac{\sigma_x + \sigma_y}{2} - \left[\left(\frac{\sigma_x - \sigma_y}{2} \right)^2 + \tau_{xy}^2 \right]^{1/2} \quad (3.59)$$

CHAPTER IV

STRESS ANALYSIS OF WELDED JOINT WITH BACKING STRIP

8.0mm thick U rib is often used but case of 6.0mm thick U-rib is sometimes acceptable to reduce weight of structures. In this study, we define 8.0mm thick U rib as Case I, and 6.0mm thick U rib as Case II.

MIDAS program, which is a commercial structural analysis program, is used and structural modeling is generated by 4 node plane stress elements. We subdivide elements at discontinuity region and the length of the model is chosen so that the effect of stress concentration diminishes.

So we define stress concentration factor (SCF) as the ratio of maximum stress to nominal stress, as follow:

$$\text{stress concentration factor} = \frac{\text{maximum stress}}{\text{nominal stress}}$$

Figure 4.1.1 shows cross section of field welded joint which is attached with backing strip and misalignment of welded joint, root gap, backing strip's dimension.

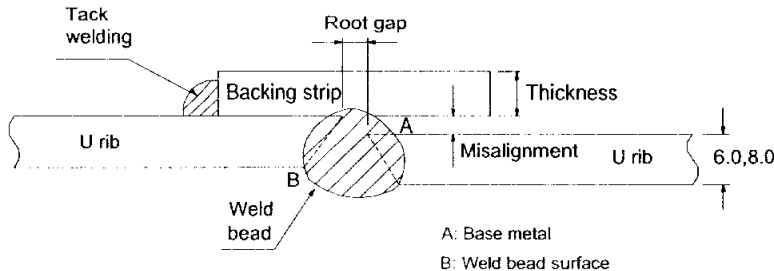


Figure 4.1.1. Cross Section of Welded Joint with Backing Strip

4.1 Case I : 8.0mm thick U rib

Stress analysis is conducted with various root shape and magnitude of misalignment due to construction error.

Also, in case of 2.0mm misalignment and right angle root, we investigate the effect of root gap and backing strip's dimension on stress behavior.

4.1.1 The relation between magnitude of misalignment and SCF

We analyse stress concentration when root gap equals 4.0mm, backing strip's thickness equals 6.0mm, backing strip's width equals 30.0mm and misalignment equals 0.0, 2.0, and 4.0mm, respectively.

A 8kgf-concentrated load is applied to end of model to create a uniform stress equaling 1 kgf/mm^2 in axial direction.

Figure 4.1.2. a), b) and c) show stress distribution corresponding to 0.0, 2.0, and 4.0mm misalignment

Those figures show that stress magnitude at root of base metal (point A) is large and stress magnitude at surface of weld bead (point B) is just a little smaller.

Figure 4.1.3 shows stress magnitude at point A and B when misalignment equals 0.0, 2.0 to 4.0mm. When magnitude of misalignment increases, stress concentration factor increases.

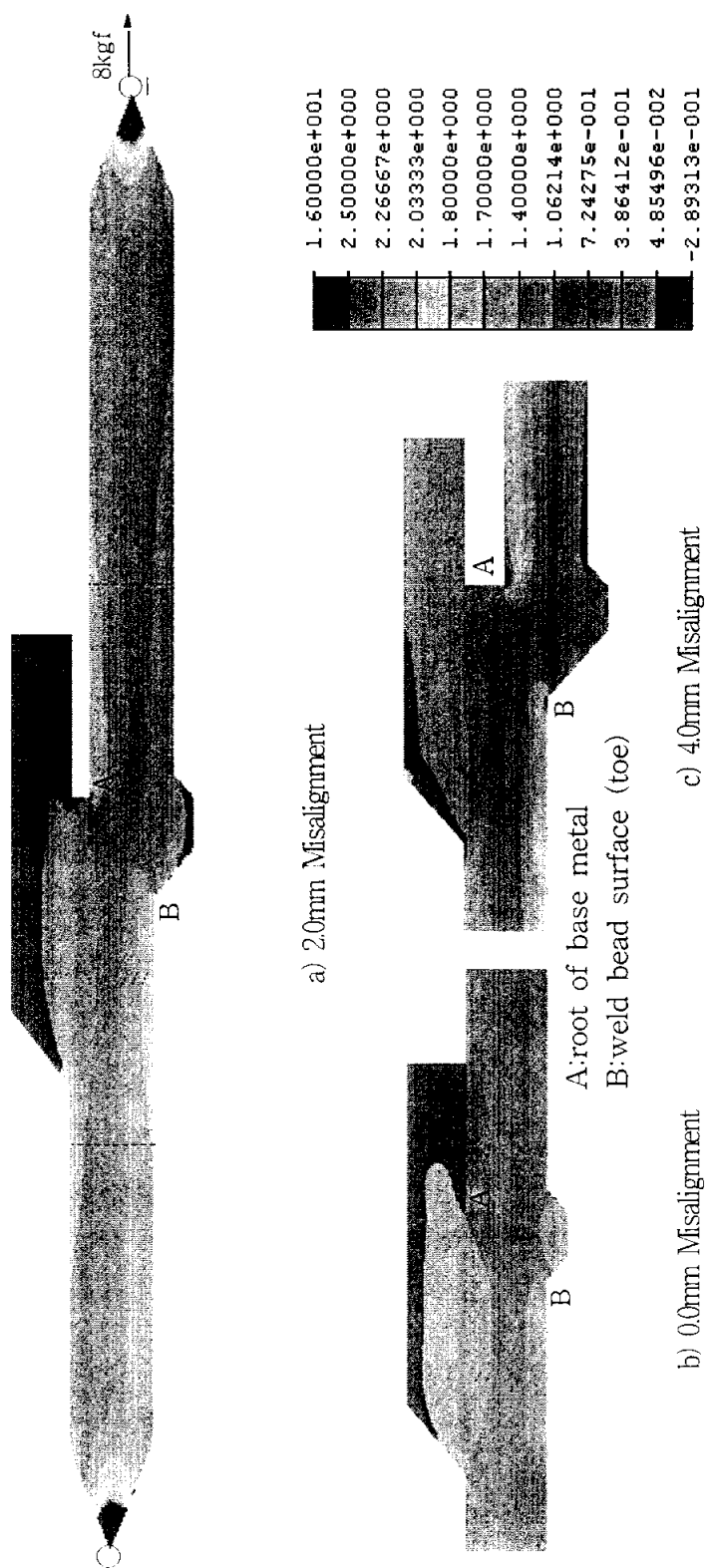


Figure 4.1.2 Analysis Model and Stress Distribution According to the Variation of Magnitude of Misalignment

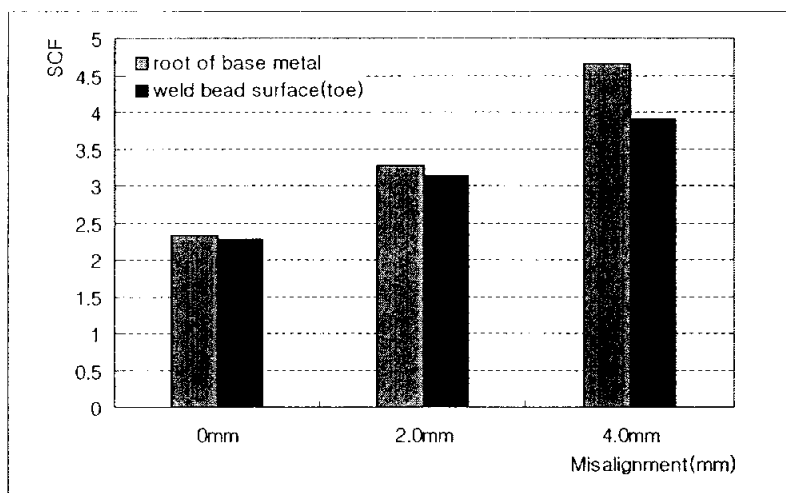
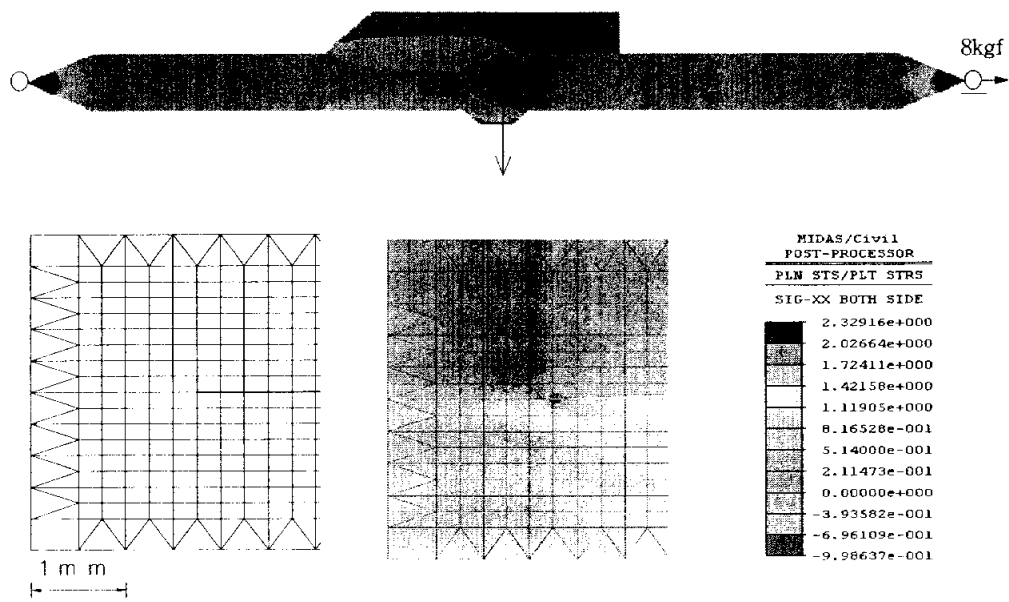


Figure 4.1.3. Relation between Magnitude of Misalignment and SCF

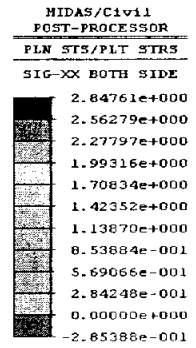
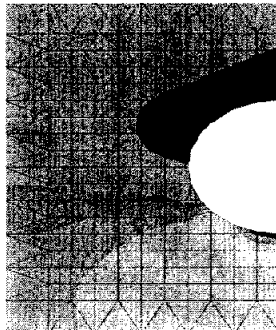
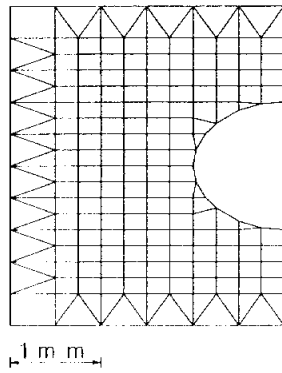
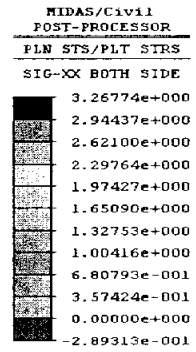
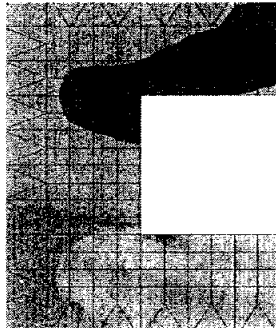
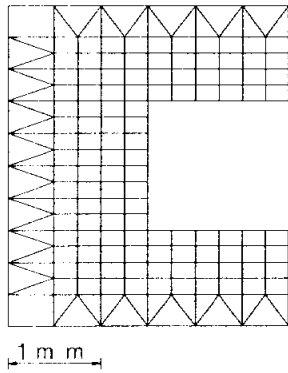
4.1.2 The relation between variation of root shape and stress concentration

We analyse stress concentration for two cases when root shape is right angle and semi-circle. In two cases modeling configurations are as follows: root gap equals 4.0mm, backing strip's thickness equals 6.0mm, backing strip's width is 30.0mm and misalignment equals 0.0, 2.0, 4.0mm, respectively.

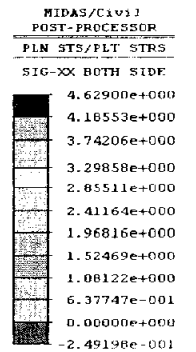
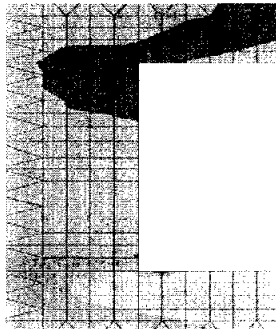
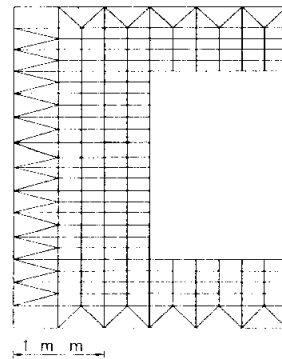
Figure 4.1.4 a), b) and c) show modeling discretization and principle stress value in case of 0.0, 2.0 and 4.0mm misalignment, respectively.

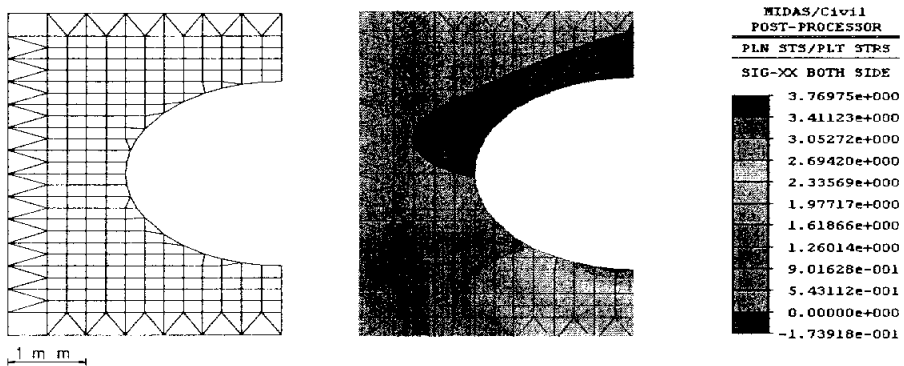


a) 0.0mm of Misalignment



b) 2.0mm of Misalignment





c) 4.0mm of Misalignment

Figure 4.1.4. Discretization of Discontinuity Region and Stress Distribution

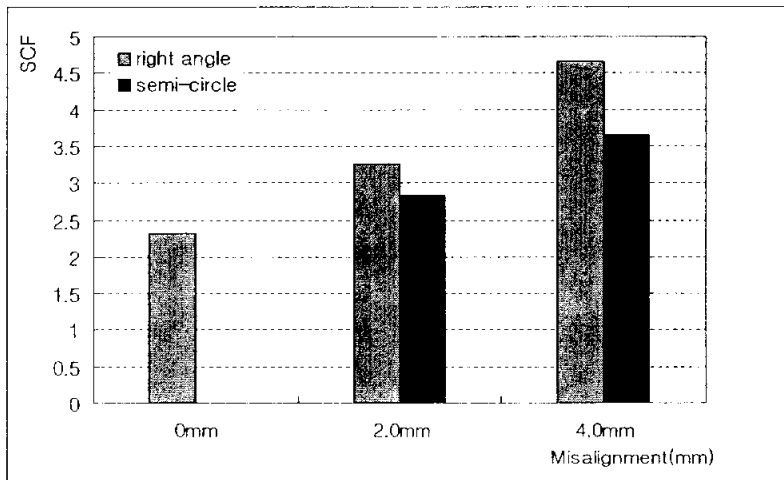


Figure 4.1.5. Relation between Root Shape and SCF

Figure 4.1.5. shows values of SCF at point A for right angle and semi circle root shape when misalignment equals 0.0, 2.0 and 4.0mm. We can see that SCF in case of right angle is bigger than that in case of semi circle.

4.1.3 The relation between root gap, backing strip's dimension and SCF

(1) The relation between root gap and SCF

We analyse stress concentration when backing strip's thickness is 6.0mm, backing strip's width is 30.0mm and root gap equals 2.0, 4.0 and 6.0mm, respectively.

As the result of analysis, stress magnitude at root of base metal (point A) is always larger than that at surface of weld bead (point B) for varied value of misalignment and root gap.

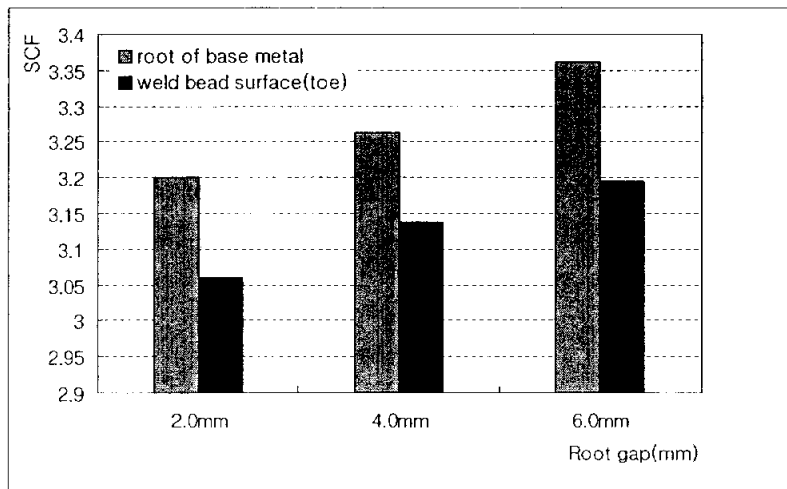


Figure 4.1.6. Relation between the Variation of Root Gap and SCF

Figure 4.1.6. shows SCF's value at point A and point B when root gap value is changed. It shows that the bigger root gap, the bigger value of SCF. Consequently, we should reduce value of root gap as small as practicable.

(2) The relation between backing strip's dimension and SCF

We analyse stress concentration for cases having root gap equals 4.0mm, backing strip's thickness is 0.0, 3.0, 6.0mm and backing strip's width is 10.0, 20.0, 30.0 mm, respectively.

The same trend as of two previous cases are obtained. It means that the stress magnitude at root gap of base metal (point A) is larger than at surface of weld bead (point B).

Figure 4.1.7 and 4.1.8 show the SCFs at point A and point B when backing strip's width and backing strip's thickness vary.

They show that backing strip's width and backing strip's thickness have no sufficient effect on SCF. Thus, we should reduce backing strip's thickness and width as small as practicable.

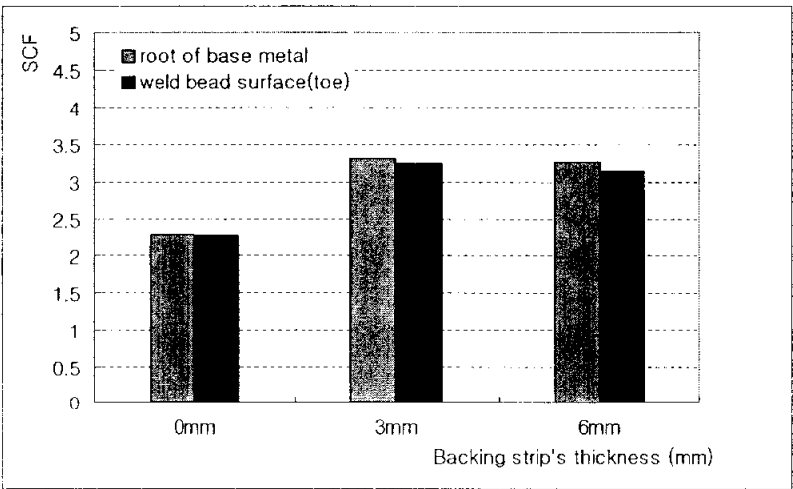


Figure 4.1.7. Relation between Backing Strip's Thickness and SCF

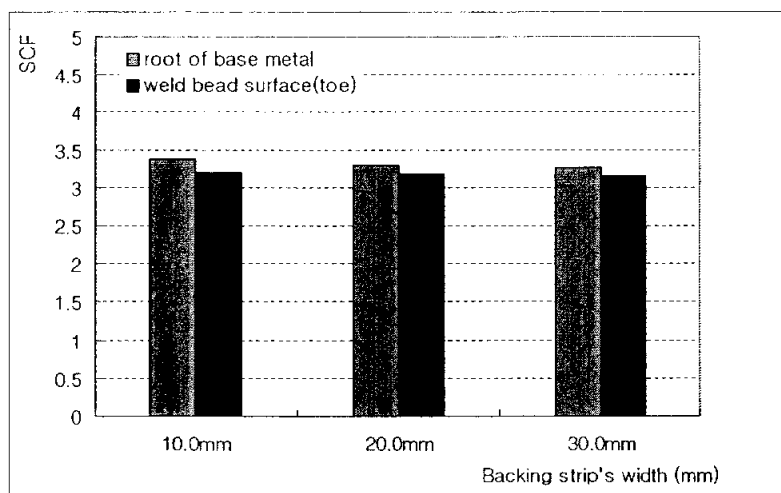


Figure 4.1.8. Relation between Backing Strip's Width and SCF

4.2 Case II : 6.0mm thick U rib

The stress behavior in this case is considered under the same conditions as of case I. A 6 kgf-concentrated load is applied at end of model to create a uniform stress equaling 1kgf/mm^2 in axial direction.

The results obtained in case II are consistent with those of case I, they also show that the stress magnitude at root of base metal (point A) is larger than that at surface of weld bead (point B) when misalignment, root gap value and backing strip's dimension vary.

4.2.1 The relation between variation of misalignment and SCF

As shown in figure 4.2.1, SCF increases rapidly when misalignment value increases from 0.0 to 1.5, and 3.0mm.

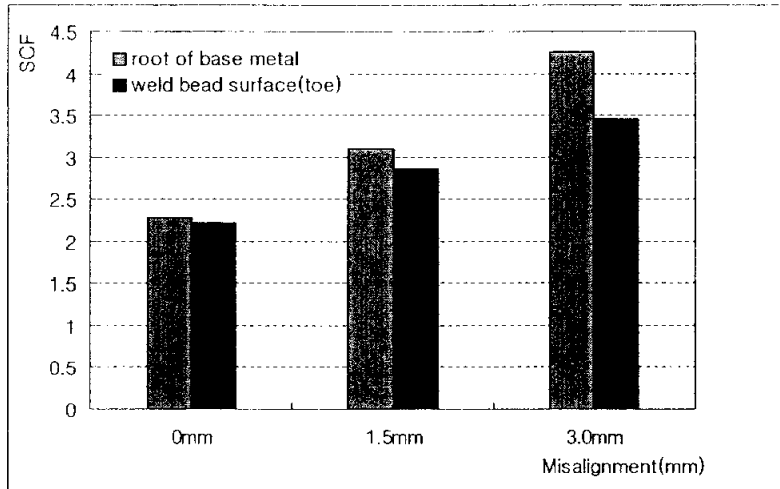


Figure 4.2.1. Relation between Magnitude of Misalignment and SCF

4.2.2 The relation between variation of root shape and SCF

Model's configurations are as follows: root gap is 4.0mm, backing strip's width is 30.0mm, backing strip's thickness is 6.0mm, and misalignment values are 0.0, 1.5, 3.0mm, respectively. We analyse stress for that model when root shape is either right angle or semi-circle.

Figure 4.2.2 shows that in case of right angle root shape, SCFs are larger than those in the case of semi-circle root shape.

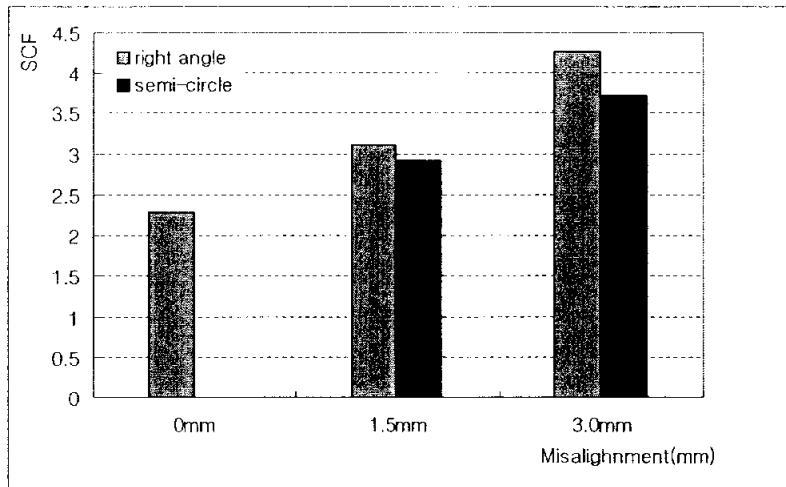


Figure 4.2.2. Relation between Root Shape and SCF

4.2.3 The relation between root gap, backing strip's dimension and SCF

(1) The relation between root gap and SCF

We study stress behavior when backing strip's thickness is 6.0mm, backing strip's width is 30.0mm and root gap value receive 2.0, 4.0, 6.0mm in turn.

Figure 4.2.3 shows that when the value of root gap is increasing, the stress concentration magnitude is increasing.

Therefore, the value of root gap should be as small as practicable.

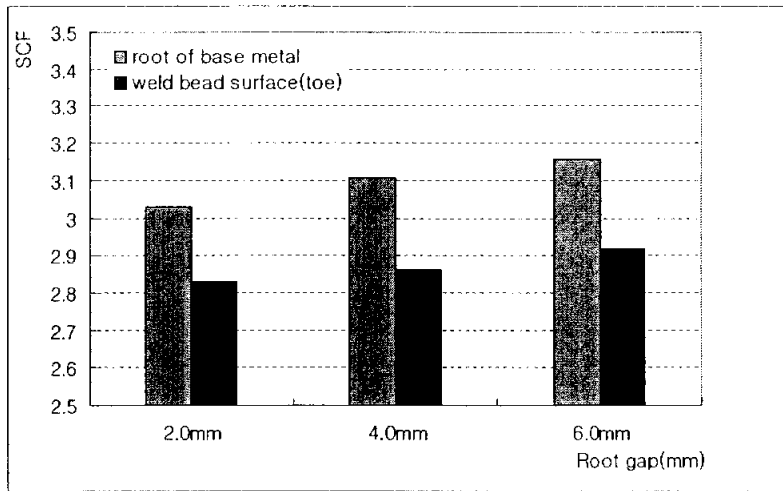


Figure 4.2.3. Relation between the Variation of Root Gap and SCF

(2) The relation between backing strip's dimension and SCF

Stress analysis is conducted when root gap value is 4.0mm, backing strip 's thickness are 0.0, 3.0, 6.0mm and backing strip's width are 10.0, 20.0, 30.0mm, respectively.

From figure 4.2.4. and 4.2.5, we know that backing strip's thickness and width have inconsiderable effect on SCF.

As the results of that, we should make backing strip's thickness and width as small as possible.

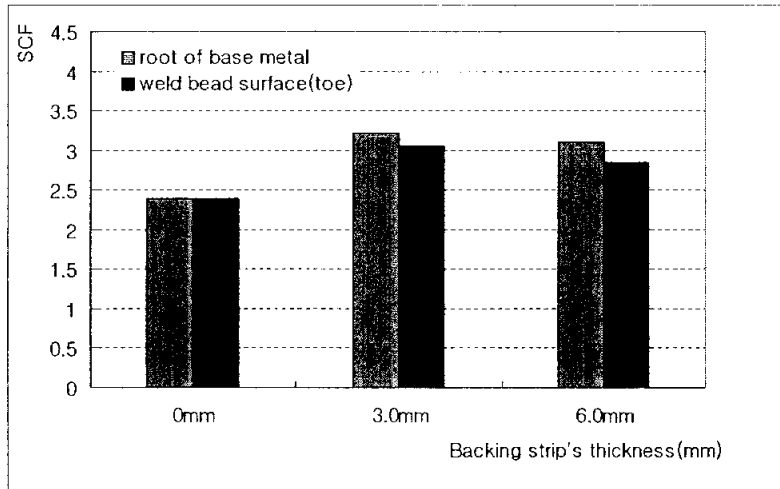


Figure 4.2.4. Relation between Backing Strip's Thickness and SCF.

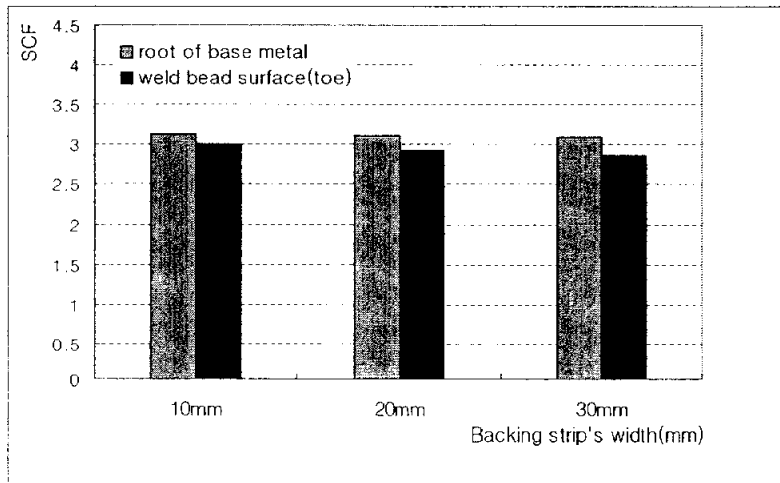


Figure 4.2.5. Relation between Backing Strip's Width and SCF

CHAPTER V

CONCLUSION

In this paper, stress analysis of welded joint with backing strip under various magnitude of misalignment, root shape, root gap and backing strip's dimension is carried out. Through this analysis, the following conclusions can be drawn:

(1) From the stress analysis results of case I and case II with various magnitude of misalignment, they show that SCF at surface of weld bead (point B) is little smaller than that at base metal (point A). Moreover, SCF increases when magnitude of misalignment increases.

Although allowable tolerance referred in AASHTO AWS D1.5 is $\delta_{\text{allowable}} = \min(\text{thickness}/10 \text{ and } 3.0\text{mm})$, I suppose that we should control misalignment δ less than 1.0mm when misalignment occurs at field in accordance with present study.

(2) For both cases, when root shape is right angle, SCF is always bigger than that in case of semi circle. Therefore, we should develop a welding method to obtain semi-circle root shape at base metal.

(3) Stress analysis is conducted when the magnitude of misalignment is fixed at 2.0mm in case I and 1.5mm in case II, and value of root gap varies from 2.0mm to 4.0mm, 6.0mm. SCF decreases when root gap decreases. We should reduce root gap as small as practicable.

According to AASHTO AWS D1.5, the minimum allowable root gap is 1/4in (6.35mm); and to Japanese Highway Bridge Code, root gap should be about 4.0~8.0mm. In addition,

according to present study, 4.0mm root gap is acceptable.

(4) Finally, backing strip's dimension has unconsiderable effect on SCF. We should reduce backing strip's dimension as small as possible. Thereby, we can reduce weight and cost of structure.

BIBLIOGRAPHIES

- Bannantine, Julie A., Jess J. Comer, and James L. Handrock. *Fundamentals of Metal Fatigue Analysis*. Prentice-Hall, 1990.
- Chitoshi, Miki, Fauzri Fahimuddin, and Kengo Anami. "Fatigue Performance of Butt-Welded Joints Containing Various Embedded Defects." *Japan Society of Civil Engineers*, vol.1, no.1, 13s-25s, (2001)
- Fisher, F. W. "Full-scale Fatigue Test of the Williamsburg Bridge Orthotropic Deck." *ASCE Structures Congress*, Proceeding vol.1, Chicago. IL (1996): 329-336.
- Fisher, J. W. *Fatigue and Fracture in Steel Bridges Case Studies*. John Wiley, New York, 1984.
- Hambly, E. C. *Bridge Deck Behavior*. E&FN SPON, 1991.
- Heins, C. P. "Bending and Torsional Design in Structural Members." Lexington, 1975.
- Ho, Choi Dong and Choi Hang Yong. "Evaluation of Fatigue Strength in Scallop at Field Bolted Joints of Longitudinal Rib and Deck Plate in Orthotropic Steel Decks." *KSSC*, vol.14, no.6 (2002): 638-690.
- Ho, Choi Dong, Choi Hang Yong, and Choi Jun Hyeok. "The Effect of Diaphragm Inside Trough Rib on Fatigue Behavior of Trough Rib and Cross Beam Connections in Orthotropic Steel Decks." *KSSC*, vol.12, no.3 (2000): 234-250.
- Howard, Cary B. *Modern Welding Technology*. Prentice Hall, 1994.

- Japan Welding Society. *Fractographic Atlas of Steel Weldments* (1983): 325-380
- Kano, T., S. Usuki, and K. Hasele. *Theory of thin-walled curved member with shear deformation*. Ingenieur-Archiv 51 (1982).
- Larry, Jeffus F. *Welding: Principles and Applications*. Delmar, 1988.
- Lee, Dong Uk. "Fundamental Study on Improvement of Fatigue Strength of Welded Joint Trough Rib for Bridge Deck Plate." Ph.D. diss. Osaka University, 1986.
- Lee, Dong Uk and Kohsuke Horikawa. "Fatigue Strength of Oneside Joint with Backing Strip." *Japan Society of Civil Engineers*, I-4, no.362 (1985): 231-237.
- Lee, Dong Uk, Kohsuke Horikawa, and Yoshiaki Arata. "Quantitative Assessment of Root Shape on Fatigue Strength of Welded Joint with Backing Strip." *Japan Welding Society*, vol.6, no.1 (1988): 158-164.
- Logan, D. L. *A First Course in the Finite Element Method*. Brooks/cole, 2002.
- Maddox, S. J. "The Fatigue Behaviour of Trapezoidal Stiffener to Deck Plate Welds in Orthotropic Bridge Deck." Department of the Environment, Supplement Report 96 UC: Crownthorne;Transport & Road Research Lab., 1974.
- Mose, F., Shiling C. G., and Raju K. S. "Fatigue Evaluation Procedure for Steel Bridge." National Cooperative Highway Research Program Report 299 (1987).

Oden, J. T. and E. A. Ripperger. "Mechanics of Elastic Structures."
Hemisphere Publishing Corporation & McGraw-Hill, 1981.

Reddy, J. N. *Theory and Analysis of Elastic Plates*. Edwards-Brothors,
1998.

Salmon, Charles C. and John E. Johnson. *Steel Structures*. Harper
Collins, 1995.

Timosenko, S. P and J. N. Goodier. *Theory of Elasticity*. McGraw-Hill
Book, 1982.

Ugural, A. C. and S. K. Fenster. *Advanced Strength and Applied
Elasticity*. Prentice-Hall PTR, 1995.

ACKNOWLEDGMENTS

I wish to express my sincere gratitude to Professor Dong Uk, Lee, my advisor, who through the years cared and helped for my Master course. I greatly appreciate his support to my study and my living by which help me overcome culture shock and fit into a foreign life.

I would like to thank to Professors of Civil Engineering Department of Pukyong National University for providing teaching, explaining and help. In particular, Professor Seung Kyu Kook and Professor Hwan Woo Lee for the helpful comments and suggestions.

I am grateful to my Korean senior, Min Su Kim, Song Min Choi, Ji Hun Song, Yong Kyo So and Korean friends. In addition, my appreciation is also expressed to Vietnamese friends who are studying at Pukyong National University.

Finally, I express my special thanks to my family, my parents, my sister, my brother, my nephew and my lover, for their many encouragements and sacrifices over the years.

Huynh Chanh Luan